PROCEEDINGS OF SCIENCE

Stochastic acceleration and the evolution of spectral distributions in SSC sources: A self consistent modeling of blazars' flares

A. Tramacere*
ISDC, University of Geneva, Chemin d' Ecogia 16, Versoix, CH-1290, Switzerland
E-mail: andrea.tramacere@unige.ch

E. Massaro

Dipartimento di Fisica, Università La Sapienza, Piazzale A. Moro 2, I-00185 Roma, Italy

A. M. Taylor

ISDC, University of Geneva, Chemin d' Ecogia 16, Versoix, CH-1290, Switzerland

Broad-band spectral distributions of non-thermal sources, such as those of several known blazars, are well described by a log-parabolic fit. The second degree term in these fits measures the curvature in the spectrum. In this paper we investigate whether the curvature parameter observed in the spectra of the synchrotron emission can be used as a fingerprint of stochastic acceleration. We use a diffusion equation in momentum space to investigate the formation of log-parabolic shape in the electron distribution, and how it's curvature is related to the diffusion term. We apply these results to some observed trends, such as the anticorrelation between the peak energy and the curvature term observed in the spectra of Mrk 421, and a sample of BL Lac objects whose synchrotron emission peaks at X-ray energies

The Extreme and Variable High Energy Sky - extremesky2011,
September 19-23, 2011
Chia Laguna (Cagliari), Italy

*Speaker.

© Copyright owned by the author(s) under the terms of the Creative Commons Attribution-NonCommercial-ShareAlike Licence.

PoS(Extremesky 2011)056

1. Introduction

In previous papers Massaro et al. (2004, 2006) found that the observed X-ray spectra of two well known HBL (High-energy peaked BL Lac) objects Mkn 421 and Mkn 501, are well described by a log-parabolic (i.e. log-normal) shape following the spectral law: $n(\gamma) = K(\gamma/\gamma_0)^{-(s+r\ \log(\gamma/\gamma_0)}$, where the term r measures the curvature of the log-parabola and s the spectral slope at the energy γ_0. A useful representation to describe log-parabolic SED in terms of it's peak energy E_s, peak height S_s, and curvature b_s is: $S(E) = S_s\ 10^{-(b_s\ \log^2(E/E_s))}$. In subsequent works, Tramacere et al. (2007, 2009); Tramacere (2007) analysed a large collection of X-ray observations of Mkn 421 and pointed out that the observed anticorrelation between b_s and E_s, could hint for a stochastic signature in the acceleration process. Tramacere et al. (2011) investigated this scenario showing that the dispersion on the fractional energy gain in each single acceleration step, is statistically equivalent to the multiplication of random variables, leading to the formation of log-normal (log-parabolic) shape of $n(\gamma)$, with r inversely proportional to the fractional energy gain dispersion. They gave a more physical description of the problem, using a diffusion equation approach, taking into account the competition between radiative losses and acceleration. Furthermore, these authors demonstrated that the inclusion of a momentum diffusion coefficient (analogous of the fractional energy dispersion), leads to the formation of log-parabolic distributions of $n(\gamma)$, and consequently, for the emitted synchrotron and inverse Compton spectra. The curvature term is inversely proportional to the diffusion-momentum term, and, as long as the acceleration times are dominating over the cooling times, the curvature of $n(\gamma)$ (and of the synchrotron emission) decreases with the time.
The presence of a momentum diffusion process is compatible with a standard diffusive shock acceleration scenario, where a turbulent magnetized medium drives the advection of particles towards the shock, and generates also a stochastic momentum diffusion. In this scenario, particles embedded in a magnetic field with both an ordered (B_0) and turbulent (δB) component, exchange energy with resonant plasma waves, and the related diffusion coefficient is determined by the spectrum of the plasma waves. Following Becker et al. (2006), the energy distribution of the magnetic turbulence $W(k)$ can be expressed in terms of the wave number $k = 2\pi/\lambda$ with a power-law: $W(k) \simeq \frac{\delta B(k_0)^2}{8\pi}\left(\frac{k}{k_0}\right)^{-q}$ with $q = 2$ for the "hard-sphere" spectrum, $q = 5/3$ for the Kolmogorov spectrum, and $q = 3/2$ for the Kraichnan spectrum. Under these assumptions the momentum-diffusion coefficient reads (O'Sullivan et al., 2009): $D_p \approx \beta_A^2\left(\frac{\delta B}{B_0}\right)^2\left(\frac{\rho_g}{\lambda_{max}}\right)^{q-1}\frac{p^2c^2}{\rho_g c}$ where $\beta_A = V_A/c$ and V_A is the Alfven velocity, $\rho_g = pc/qB$ is the Larmor radius, and λ_{max} is the maximum wavelength of the Alfven waves spectrum. The momentum-diffusion coefficient can be expressed as a power-law in terms of the Lorentz factor γ, $D_p(\gamma) = D_{p0}(\gamma/\gamma_0)^q$. We address the reader to Tramacere et al. (2011) to have more detailed and insightful description of the topic. In this paper we focus on how the E_s-b_s and the E_s-S_s trends, observed in the synchrotron emission of some HBLs, can be reproduced by a stochastic acceleration scenario.

2. Spectral evolution of high energy flares of bright HBL objects

The analysis of Tramacere (2007) and Tramacere et al. (2007, 2009) on the synchrotron SED of Mkr 421 showed an anticorrelation between E_s and b_s and an interesting correlation between E_s and S_s. Massaro et al. (2008) found that the E_s-b_s and E_s-S_s trends hold also for a larger sample

PoS(Extremesky 2011)056

of eleven HBLs, making stronger the hypothesis that a common accelerative mechanism may drive such physical processes for this class of active galactic nuclei. It is useful to report the expected trend for E_S and S_S (Tramacere et al., 2009) based on the δ-function approximation of the standard synchrotron theory (e.g. Rybicki & Lightman (1986)): $S_s(E_s) \propto n(\gamma_{3p})\gamma_{3p}^3 B^2\delta^4$ and $E_s \propto \gamma_{3p}^2 B\delta$, where γ_{3p} represents the peak of $\gamma^3 n(\gamma)$, implying a power-law trend for S_S-E_S:

$$S_s \propto (E_s)^{\alpha}, \tag{2.1}$$

where $\alpha = 1.5$ applies for changes of γ_{3p} leaving constant $n(\gamma_{3p})$, $\alpha = 2$ for variations of B only, and $\alpha = 4$ when the main driver is δ. The peak energy γ_{3p}, when $n(\gamma)$ has a log-parabolic shape, reads: $\log(\gamma_{3p}) = \log(\gamma_p) + \frac{3}{2r}$. Using the relation $b_s \simeq r_{3p}/5$ (Massaro et al., 2004), (where r_{3p} represents the curvature at of $n(\gamma)$ at γ_{3p}.), it follows: $\log(E_s) \propto 2\log(\gamma_p) + \frac{3}{5b_s}$, hence the relation between b_s and E_s is:

$$b_s = \frac{a}{\log(E_s/E_0)} \tag{2.2}$$

with $a = 3/5 = 0.6$. Eq. 2.2, tells us that a decrease in the curvature leads to an increase in E_p (and γ_{3p}). Hence, variations of the diffusion momentum term leading to broader spectra (lower values of r and b_s), should results in larger values of E_S. Of course, an increase in γ_{3p} will lead to an increase in S_S (Eq. 2.1), as long as variations of γ_{3p} dominate over simultaneous variations of B, $n(\gamma_{3p})$, and δ.

To give a theoretical framework to the phenomenological relations reported in Eq. 2.1 and 2.2, we try to reproduce both the E_s-b_s and E_s-S_s trends using a stochastic acceleration scenario. In the following we will consider the data of Mrk 421 from Tramacere et al. (2007, 2009), collected over a period of 13 years, and of six HBL objects from Massaro et al. (2008): Mrk 180, Mrk 501, PKS 0548-322, PKS 1959-650, 1H 1426+428, covering a period of about 11 years and including both quiescent and flaring states. We consider two scenarios. In the first case, we assume variations of D_{p0}, due to changes of $\delta B/B$ or β_A, but $q = 2$ remains stable. In the second scenario q is ranging in the interval [3/2, 2], and D_{p0} is fixed. We describe the temporal evolution of $n(\gamma)$ by solving the governing continuity equation for each value of D_p (or q), and for three values of the magnetic field B = 0.05, 0.1, and 0.2 (G). For each temporal evolution we compute the averaged SEDs of both the synchrotron and inverse Compton components. During the temporal evolution of duration T, particles are injected for a time T_{inj}, with a quasi-mono energetic spectrum (γ_{inj}), and with an injected luminosity of L_{inj}. Particles are continuously accelerated due to a momentum diffusion process with an acceleration time $t_{D0} = 1/D_{p0}$, and by a systematic process with an acceleration time t_A. They also suffers radiative cooling through synchrotron and inverse Compton mechanisms. Particle escape is taken into account by the energy independent escape time T_{esc}: all these parameters are summarised in Tab. 1. The comparison with the data can be affected by an observational bias due to the limited energy range of detectors. In fact, when the peak energy is close to the range boundaries, the curvature is not well estimated because one can use only a portion of the parabola below or above the peak. Generally, curvatures lower than the actual ones are obtained. The energy range [0.5, 100.0] keV is the typical spectral window covered by X-ray and hard-X-ray detectors. In our analysis we used this fixed window to take into account this possible bias in the observed data when E_s is variable.

PoS(Extremesky 2011)056

Table 1: Parameters' values adopted in the numerical solutions of the diffusion equation to reproduce the observed trends of the HBLs reported in the figures.

		D trend	q trend
R	(cm)	3×10^{15}	-
B	(G)	[0.05-0.2]	-
L_{inj} (E_s-b_s trend)	(erg/s)	5×10^{39}	-
L_{inj} (E_s-L_s trend)	(erg/s)	$5\times10^{38}, 5\times10^{39}$	-
q		2	[3/2-2]
t_A	(s)	1.2×10^{3}	-
$t_{D_0}=1/D_{P0}$	(s)	$[1.5\times10^{4}-1.5\times10^{5}]$	1.5×10^{4}
T_{inj}	(s)	10^{4}	-
T_{esc}	(R/c)	2.0	-
T	(s)	10^{4}	-
γ_{inj}		10.0	-

2.1 E_s-b_s relation

The E_s-b_s anticorrelation is the strongest signature of a stochastic component in the acceleration. In Fig. 1 we report the scatter plot in the E_s-b_s plane for the six considered sources. The left panel reports the results obtained by changing the value of D_{p0}: the green dashed lines describe the trend resulting from a log-parabolic fit of the synchrotron SED over a decade in energy centered on E_s; the purple lines represent the same trend obtained by fitting log-parabola in the fixed spectral window [0.5, 100.0] keV. Both these trends are compatible with the data and track the predicted anticorrelation between E_s and b_s. Purple data, however, give a better description, hinting that the "window" effect could be a real bias. Each of the three lines was computed for a different value of B. It is remarkable that the variation of a single parameter, D_{p0} can describe the observed behaviour. The dispersion in the data is relevant, and can be related to the variation of B (as partially recovered by numerical computation), or by different values of the beaming factor δ, the source size R and the injection energy rate L_{inj} in the various flares of these objects.

The dot-dashed tick line represents the best fit of the observed data by means of Eq. 2.2, and returns a value of $a\approx0.6$, as expected from theoretical predictions for the case of the δ-approximation, and pure log-parabolic electron distribution. This fitted line is also compatible with the numerical trend shown by the purple lines. Note that the observed curvature values are in the range [0.1, 0.5], corresponding to $r_{3p}\sim$ [0.5, 3.0]. According to the results presented in Tramacere et al. (2011), the expected equilibrium curvature in the synchrotron emission, in the full Klein-Nishina or Thomson inverse Compton regime, and for $q=2$, should be of $r_{3p}\approx6.0$, and of $r_{3p}\approx5.0$ in the intermediate regime. In the case of $q=3/2$, the equilibrium curvature should be $r_{3p}\sim3.0$. This is perhaps an interesting hint that, both in flaring and quiescent states, for $q=2$, the distribution is always far from equilibrium. In the case of $q=3/2$, only for $E_s\lesssim1.5$ keV the curvature are compatible with the equilibrium ($r_{3p}\simeq3.0$, corresponding to $b_s\sim0.6$). For larger values of E_s, we find again curvatures well below the equilibrium value. These results provide a good constraint on the values of the magnetic field $B\lesssim0.1$ G. The q-driven trend (right panel) is also compatible with the data, but for values of $E_s\lesssim1$ keV, the D_{p0}-driven case seems to describe

PoS(Extremesky 2011)056

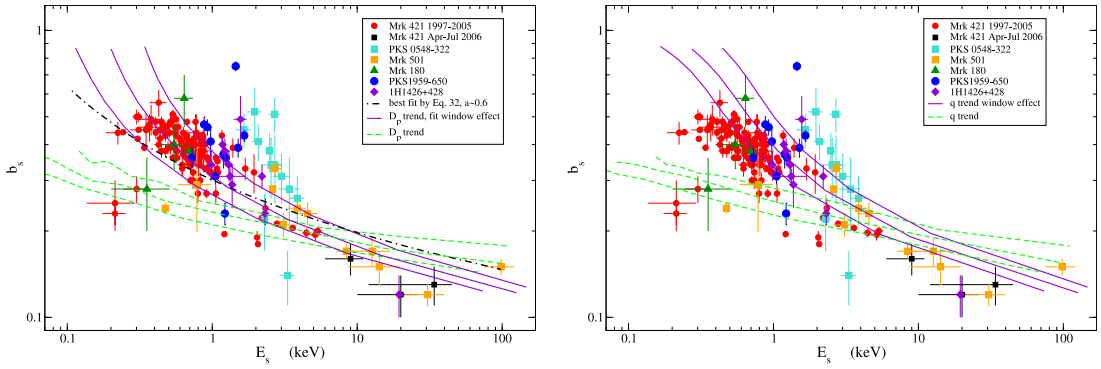

Figure 1: *Left panel:* the E_s-b_s trend observed for the six HBLs in our sample. The dashed green lines represent the trend reproduced by stochastic acceleration model, for the parameters reported in Tab. 1, and for the D trend, the different lines corresponding to three different values of B reported in Tab. 1. The purple lines represent the trend obtained by fitting the numerically computed SED over a fixed spectral window in the range $0.5-100$ keV. *Right panel:* the same as in the left panel for the case of the q trend.

better the observed behaviour, but any firm conclusion is not possible because of the dispersion of the data.

2.2 E_s-L_s trend

As a last benchmark for the stochastic acceleration model, we reproduce the observed correlation between E_s and S_s, which follows naturally from the variations of D_{p0} and q. Considering that the redshifts of the six considered HBL objects are different, we prefer to use their peak luminosity $L_s = S_s\ 4\pi\ D_L^2$, where D_L is the luminosity distance [1]. To account for the different jet power of sources, we considered two data subsets, and we assumed $L_{inj} = 5 \times 10^{39}$ erg/s for the first subset (top panels of Fig. 2), and $L_{inj} = 5 \times 10^{38}$ for second (bottom panels of Fig. 2). In the left panels of Fig. 2, we report the D_{p0} driven trend, and in the right panels the q driven trend. Solid lines represent the trend obtained by deriving L_s from the log-parabolic best fit of the numerically computed SEDs, centered on E_s; dashed lines are the trends obtained by fitting the numerical results in the fixed energy window [0.5, 100] keV. Both the results give a good description of the observed data, and their shapes are similar. Solid lines follow well a power-law with an exponent of about 0.6, while the windowed trends (dashed lines) show a break around 1 keV and the exponent below this energy turns to about 1.5. The exponent of 0.6 is softer than the value of 1.5 predicted in the case of $\delta-$approximation and $n(\gamma_{3p}) = \text{const}$, and compatible with a constant value of L_{inj} (Tramacere et al., 2011). A similar break at the same energy, can be noticed in the points of Mrk 421 in the E_s-S_s plot presented by Tramacere et al. (2009), who found an exponent of $\sim$ 1.1 and of $\sim$0.4 below and above 1 keV, respectively.

3. Conclusions

The comparison of the E_s-b_s and E_s-S_s trends, obtained through several X-ray observations of six HBL objects spanning a period of many years, with those predicted by the stochastic acceleration model, shows very good agreement. We are able to reproduce these long-term behaviours,

[1] We used a flat cosmology model with: H_0= 73 km/s/Mpc, Ω_{matter}=0.27, Ω_{vacuum} = 0.73

PoS(Extremesky 2011)056

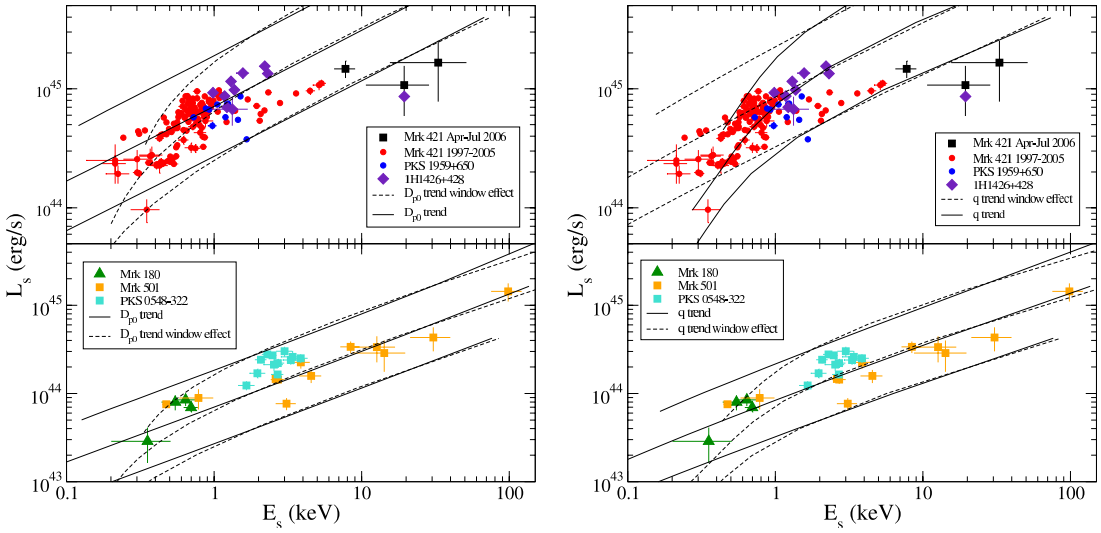

Figure 2: *Left panels:* the E_s-L_s trend observed for six HBLs in our sample, top panel corresponds to the case of $L_{inj} = 5 \times 10^{39}$ erg/s, bottom panel corresponds to the case of $L_{inj} = 5 \times 10^{38}$. The solid black lines represent the trend reproduced by stochastic acceleration model, for the parameters reported in Tab. 1, and for the D trend, the different lines corresponding to three different values of B reported in Tab. 1. The dashed lines represent the trend obtained by fitting the numerically computed SED over a fixed spectral window in the range $0.5 - 100$ keV. *Right panels:* the same as in the left panel for the case of the q trend.

by changing the value of only one parameter (D_{p0} or q). Interestingly, the E_s-S_s relation follows naturally from that between E_s and b_s. This result is quite robust and hints at a common accelerative scenario acting in the jets of HBLs. As a last remark, we note that recently Massaro & Grindlay (2011) find also in the case of GRBs a E_s-b_s trend, similar to that observed in the case of HBL objects. They measured values of the curvature up to 1.0, typically higher than in HBLs. It's interesting to note that the value of 1.0 is close to the limit of $\sim$1.2, that we predict in the case of distributions approaching the equilibrium for inverse Compton scattering with $q = 2$.

References

Becker, P. A., Le, T., & Dermer, C. D. 2006, The Astrophysical Journal, 647, 539

Massaro, E., Perri, M., Giommi, P., & Nesci, R. 2004, Astronomy and Astrophysics, 413, 489

Massaro, E., Tramacere, A., Perri, M., Giommi, P., & Tosti, G. 2006, Astronomy and Astrophysics, 448, 861

Massaro, F., & Grindlay, J. E. 2011, ApJ 727L 1

Massaro, F., Tramacere, A., Cavaliere, A., Perri, M., & Giommi, P. 2008, Astronomy and Astrophysics, 478, 395

O'Sullivan, S., Reville, B., & Taylor, A. M. 2009, Monthly Notices of the Royal Astronomical Society, 400, 248

Rybicki, G. B., & Lightman, A. P. 1986, Radiative Processes in Astrophysics, iSBN: 0-471-82759-2

Tramacere, A. 2007, Ph.D. Thesis, Spectral Variability in Blazar's High Energy Emission, La Sapienza University, Rome, 1

Tramacere, A., Giommi, P., Perri, M., Verrecchia, F., & Tosti, G. 2009, Astronomy and Astrophysics, 501, 879

Tramacere, A., Massaro, F., & Cavaliere, A. 2007, Astronomy and Astrophysics, 466, 521

Tramacere, A., Massaro, E., & Taylor, A. M. 2011, Astrophysical Journal, 739, 66

PoS(Extremesky 2011)056